Journal of Materials Chemistry C

Accepted Manuscript

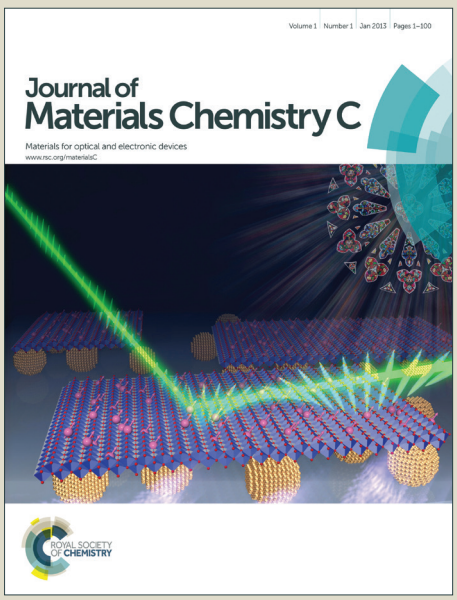

ROYAL SOCIETY OF CHEMISTRY

www.rsc.org/materialsC

Cite this: DOI: 10.1039/c0xx00000x

www.rsc.org/xxxxxx

ARTICLE TYPE

Improved synthesis and photovoltaic performance of donor-acceptor copolymers based on dibenzothiophene-cored ladder-type heptacyclic units

Lixin Wang,[ab] Dongdong Cai,[a] Changquan Tang,[a] Meng Wang,[ab] Zhigang Yin[ab] and Qingdong Zheng*[a]

Received (in XXX, XXX) Xth XXXXXXXXX 20XX, Accepted Xth XXXXXXXXX 20XX
DOI: 10.1039/b000000x

We have developed a facile synthetic route to a ladder-type donor unit (SDCT) wherein two outer thiophene subunits are covalently fastened to the central dibenzothiophene core through two sp^3-hybridized bridging carbons. An innovative transformation from an aryl ketone group to an aryl ester group was applied to construct the ladder-type molecular skeleton, and the overall synthetic yield toward the donor unit has been significantly improved by choosing aryl side chains instead of aliphatic ones to avoid competing dehydration reactions. To reveal the effects of π-spacers and heteroatom substituents, three donor-acceptor (D-A) copolymers containing SDCT and acceptor units of 2,1,3-benzothiadiazole (BT), 2,1,3-benzoxadiazole (BO), or 4,7-bis(2-thienyl)-2,1,3-benzothiadiazole (DTBT) were synthesized, characterized and used for polymer solar cells (PSCs). All polymers exhibit blue-shifted absorption spectra and deeper-lying HOMO energy levels compared to the previous carbazole-based skeleton analogues. In comparison with its analogous polymer with the same π-conjugated backbone, the polymer with alkoxy-substituted BT as the acceptor unit (PSBT) shows an order of magnitude higher OFET mobility (1.8×10^{-4} *versus* 1.25×10^{-5} cm^2 V^{-1} s^{-1}). An optimal device based on PSBT:$PC_{71}BM$ (1/3 in wt%) delivers a respectable PCE of 5.18% and a high V_{oc} of 0.94 V. All of which are superior to those of the carbazole-based analogue (PCE = 3.7%, V_{oc} = 0.80 V) and greatly surpass the values of the previous dibenzothiophene-based polymer (PCE = 0.76%, V_{oc} = 0.64 V). These results demonstrate that SDCT is a promising building block for constructing photovoltaic polymers and the synthetic strategy developed herein can be used to prepare other dibenzothiophene-cored ladder-type heptacyclic units.

Introduction

Light weight, mechanical flexibility, large-area compatibility, earth-abundant constituents and cost-effective solution processing of polymer solar cells (PSCs) have triggered increasing research efforts in new material innovation,[1] novel device architectures,[2] various interfacial engineering,[3] and morphology control.[4] Among the aforementioned efforts to improve the performance of PSCs, the active-layer material innovation, especially *p*-type conjugated copolymers, is vital for efficient PSCs.[5] Typically, benzodithiophene (BDT)-based polymers have contributed to single-junction PSCs with power conversion efficiencies (PCEs) over 10%,[6] which significantly outperformed that of other thoroughly investigated polymers such as poly(3-hexylthiophene) P3HT.[7] To explore novel *p*-type polymer materials toward an enhancement in PCE, the donor-acceptor (D-A) approach which alternates electron-rich and electron-deficient moieties along the polymer backbone is one of the most successful and universal strategies, because it enables tunable absorption spectra and tailored frontier molecular orbital energy levels of the resulting polymers through meticulously screening different donor segments as well as various acceptor units. Although integrating the existing building blocks into new copolymers is an effective way to synthesize new materials, exploring novel structural units to construct high performance polymers is even desirable from the viewpoint of molecular design.

Poly[N-9'-heptadecanyl-2,7-carbazole-*alt*-5,5-(4',7'-di-2-thienyl-2',1',3'-benzothiadiazole)] (PCDTBT) is an excellent example of polymers based on N-alkyl-2,7-carbazole, and PCDTBT has been used as an active layer material in more than 250 publications.[8] However, the number of carbazole-derived high-performance polymers for PSCs is relatively limited.[9] Ladder-type building blocks with multi-ring-fused structures are promising donor constituents for photovotaic copolymers, because the planar multi-ring-fused aromatics can facilitate π-electron delocalization and elongate effective π-conjugation that is favorable for bandgap reduction.[10] At the same time, the planar aromatics tend to pack closely in solid state through strong intermolecular π-π stacking, endowing the film with good charge transport property. Previously, we synthesized a copolymer based on a ladder-type heptacyclic unit which is derived from carbazole (PHHA-BT in Scheme 1).[11] When its analogous polymer (PCDCTBT-C8, Scheme 2) was used for PSCs, a moderate PCE had been achieved.[12] On the other hand, it is known that bridging

Cite this: DOI: 10.1039/c0xx00000x

www.rsc.org/xxxxxx

ARTICLE TYPE

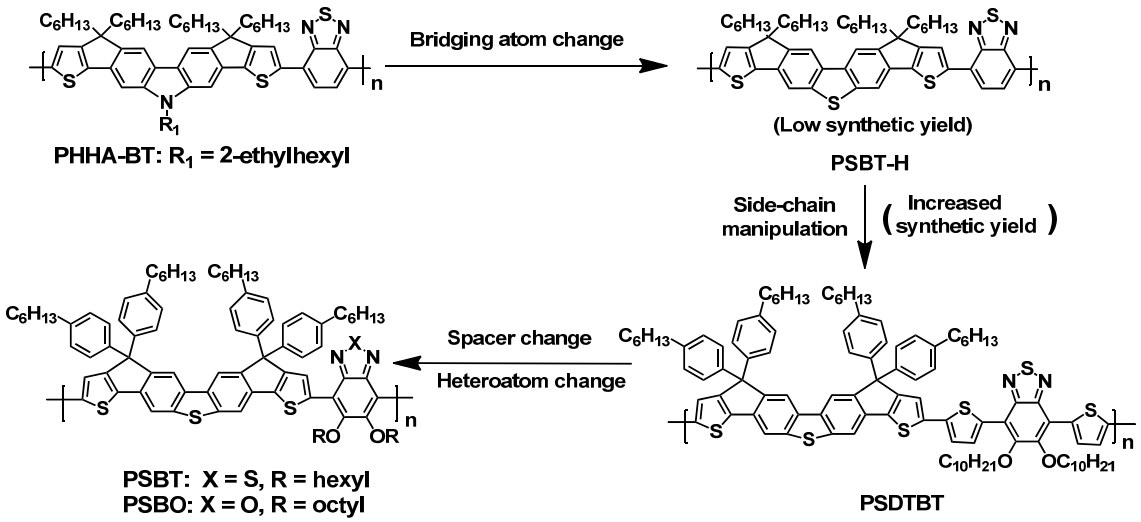

Scheme 1 Molecular design strategies for the dibenzothiophene-based donor units and copolymers.

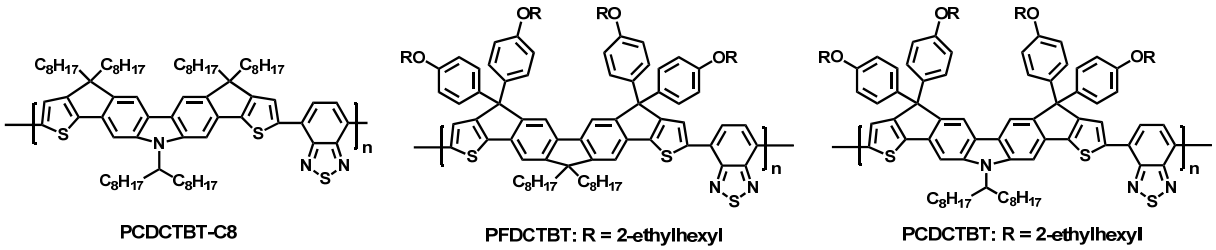

Scheme 2 Chemical structures of some reported copolymers based on carbazole- or fluorene-derived heteroheptacenes.

atoms also play key roles in determining the final photovoltaic properties of the resulting polymers.[13] Subsequently, we developed another series of copolymers based on a ladder-type heteroheptacene which is derived from dibenzothiophene (such as PSBT-H in Scheme 1),[14] wherein the N-atom of carbazole in PHHA-BT was solely replaced by the S-atom. Unfortunately, the key two-step cyclization reaction occurred with a low yield of 13%, leading to an overall yield of only 9% from the starting material of 3,7-dibromodibenzo[b,d] thiophene to the brominated heptacyclic donor unit. Moreover, although a PCE of 4.17% was eventually achieved based on a "donor-donor" conjugated copolymer that incorporates bithiophene as the other repeat unit, the D-A copolymer using benzothiadiazole as an acceptor unit only delivered a relatively low PCE of 0.69%.[14]

In order to improve the reaction yield of the two-step alcoholization/annulation cyclization, in this report we circumvent the utilization of alkyl side chains that would lead to olefine by-products *via* a competing dehydration reaction of the intermediate tertiary alcohol.[12] Alternatively, 4-hexylphenyl groups are applied as the solubilizing side-chain sources.[15] Consequently, the two-step cyclization procedure proceeded smoothly in 60% yield (Scheme 3), and the overall yield from the starting material of 3,7-dibromodibenzo[b,d]thiophene to the brominated heptacyclic donor unit is improved from 9% to 35%. Therefore, adequate brominated donor molecules can be easily produced, followed by one more step of reaction to efficiently afford the distannyl monomer. Subsequently, the distannyl donor monomer can be copolymerized with various halogenated acceptor moieties.[16] It is worth noting that the rigid and planar ladder-type backbones are usually obtained through an ester functional group mediated two-step alcoholization/annulation procedure besides the complicated three-step acylation/reduction/alkylation sequence.[12, 17] However, it is synthetically challenging to directly attach ester groups to the desirable positions on an aromatic moiety. To solve this problem, we conceived an indirect presursor solution, namely, converting aromatic methyl ketones into formic acids *via* aq. NaClO mediated haloform reactions. As for the acceptor unit, the classic building block of 4,7-bis(2-thienyl)-2,1,3-benzothiadiazole (DTBT) was chosen. The insertion of two additional thiophene

Cite this: DOI: 10.1039/c0xx00000x

www.rsc.org/xxxxxx

ARTICLE TYPE

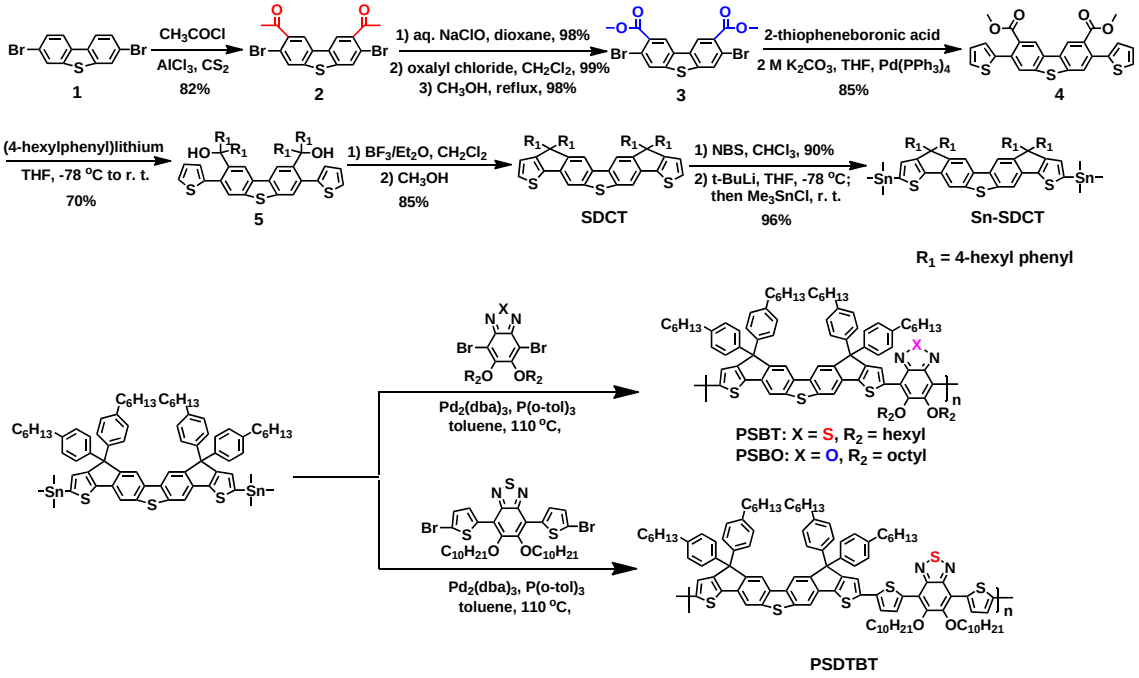

Scheme 3 Synthesis of the monomers and polymers with varying acceptor moieties.

rings between the BT unit and the donor unit usually serves to relieve the torsional disorder along the polymer backbone, which is favorable for the conjugation extension. However, due to the electron-rich nature of thiophene, it will result in an undesirable reduction in ionization potential of the polymer and therefore the open-circuit voltage (V_{oc}).[18] Thus the single BT acceptor motif without the flanking thiophenes is more promising in terms of a high V_{oc}. In addition, 2,1,3-benzoxadiazole (BO) obtained by replacing the sulfur atom in BT unit with an oxygen atom, is favorable for reducing the HOMO level of the resulting polymer in some cases.[19] Therefore, the polymer using BO as the acceptor unit is also prepared for a comparison purpose. As such, three dibenzothiophene-based polymers, i.e., PSDTBT, PSBT and PSBO (Scheme 1), are synthesized and tested for PSCs. Finally, optimal devices based on PSBT exhibit a PCE over 5.1% with a high V_{oc} of 0.95 V, all of which are superior to those of the carbazole- or fluorene-derived photovoltaic polymers (PCDCTBT and PFDCTBT, Scheme 2) which have similar backbone units.[20] Moreover, the values of PCEs and V_{oc}s obtained herein are far more than those of the previous work (PCE_{max} = 0.76%, V_{oc} = 0.64 V) based on the ideal polymer skeleton (PSBT-H, in Scheme 1).[14] These results highlight that the new ladder-type dibenzothiophene-cored multi-fused heptacyclic unit (SDCT) is a promising building block for high-performance polymers, and the synthetic procedure developed herein is an effective strategy to prepare SDCT and its derivatives. At the same time, the methyl ketone groups are first used as precursors of ester moieties to construct ladder-type multi-fused polycyclic units.

Results and discussion

Synthesis and characterization

To guarantee adequate solubility of the resulting polymers, alkoxy BT/BO acceptor moieties were applied, and the 4,7-bis(5-bromothiophen-2-yl)-5,6-bis(decyloxy)-2,1,3-benzothiadiazole (DTBT-OC_{10}), 4,7-dibromo-5,6-bis(hexyloxy)-2,1,3-benzothiadiazole (BT-OC_6) and 4,7-dibromo-5,6-bis(octyloxy)-2,1,3-benzoxadiazole (BO-OC_8) units with different side chains were synthesized according to the previously reported procedures.[21] The synthetic routes of the distannyl donor monomer and the three copolymers are depicted in Scheme 3, and the detailed experimental procedures are given in the Experimental Section. Starting from 3,7-dibromodibenzo[b,d]-thiophene (**1**), double Friedel-Crafts acylation using acetyl chloride with the aid of $AlCl_3$ in carbon disulfide yielded compound **2**. NaClO (bleach) mediated haloform reaction of the methyl ketone groups in compound **2** proceeded smoothly to furnish an intermediate of diacid in a high yield of 98%, which was followed by reacting with oxalyl chloride to afford diacid chlorides and then subjected to react with methanol to obtain a diester (**3**). Stille coupling reaction between **3** and 2-thiopheneboronic acid was performed in the presence of $Pd(PPh_3)_4$ with aq. K_2CO_3/THF as the solvent to afford compound **4** with a yield of 85%. Subsequently, nucleophilic attacks at the carbonyl site of compound **4** by freshly prepared (4-hexylphenyl)lithium produced a crude diol (**5**), which underwent cyclization with boron trifluoride–etherate to give the

key heptacyclic arene (SDCT) in 60% overall yield. Finally, SDCT was converted to a dibrominated intermediate (Br-SDCT) which was efficiently lithiated by *t*-butyllithium and then followed by quenching with trimethyltin to accomplish the donor monomer (Sn-SDCT) synthesis. Three D-A copolymers (PSBT, PSBO and PSDTBT) were generated by Stille coupling between the Sn-SDCT donor monomer and BT-OC_6, BO-OC_8, and DTBT-OC_{10} acceptor monomers, respectively. All polymers were purified by Soxhlet extraction with methanol, acetone and hexane eluents successively to remove oligomers and the residual catalyst. The purified polymers show good solubility in common organic solvents, such as chloroform, toluene and dichlorobenzene. Gel permeation chromatography (GPC) results show that the number-average molecular weights (M_n) and polydispersity indices (PDIs) of PSBT, PSBO, and PSDTBT are 7.6 kDa (PDI = 1.3), 7.7 kDa (PDI = 1.8), and 5.3 kDa (PDI = 1.7), respectively (Table 1). The relatively low molecular weights observed for these polymers may be related with the great steric hindrance posed by the bulky aryl side chains in the donor unit and long alkyl chains in the acceptor units, that would restrain close molecular collisions during the chain propagation. Thermogravimetric analysis (TGA) under nitrogen suggests that all polymers are favorably stable for PSCs with the 5% weight-loss temperatures (T_d) of 315, 309 and 320 °C for PSBT, PSBO and PSDTBT, respectively (Fig. 1). X-ray diffraction measurements for the pristine thin films of these copolymers reveal no peak signal between $2\theta = 2.5^o$ and 20^o which indicates their amorphous features (Fig. S2).

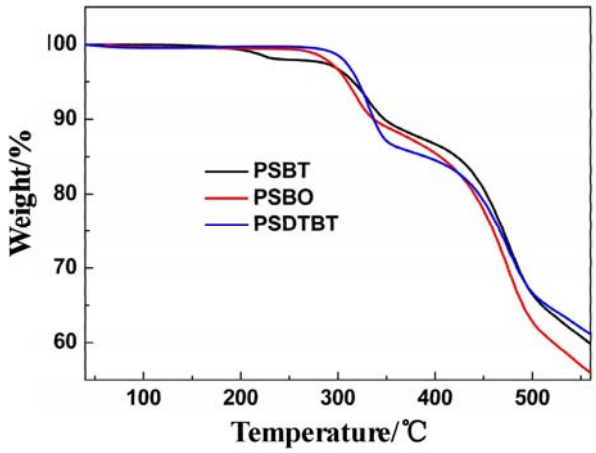

Fig. 1 TGA plots of the three polymers with a heating rate of 10 °C/min under N_2 atmosphere.

Optical properties

UV-vis absorption spectra of the three polymers in dilute CB solution and in thin film are shown in Fig. 2, and the relevant data are listed in Table 1. Both in solution and in the solid state, two main absorption bands are observed which is typical for D–A copolymers. The lower energy absorbance comes from the intramolecular charge transfer (ICT) between the donor and acceptor units, while the shorter wavelength band is attributed to π–π* transition of the heteroheptacene. Compared to the absorption spectra in solution, three copolymers show nearly unchanged π–π* transition bands in the solid state. While the ICT profiles of PSDTBT shift toward longer wavelengths from solution to the solid state, the absorption maxima of ICT bands in the film spectra of PSBT and PSBO, however, exhibit blue-shifts of 5 and 19 nm, respectively, compared to those in solution. It may be attributed to the steric hindrance between the pendent phenyl rings on the SDCT unit and the side chains on the BT/BO unit that may dilute strong intermolecular π–π interactions.[22] The absorption maxima of PSBT and PSBO in solution at longer wavelength regions indicate that the acceptor strength of BO is stronger than that of BT. Compared to PSBT, PSDTBT with two flanking thiophene rings in the acceptor unit shows a red-shifted π–π* transition band due to the longer conjugated length. However, this modification also leads to a blue-shift of the ICT band due to the weaker donor-acceptor interactions. Optical bandgaps (E_g^{opt}) deduced from the absorption edges of the thin film spectra were determined to be 1.81 eV for PSBT and 1.82 eV for both of PSBO and PSDTBT. In comparison with their carbazole-based skeleton analogues (Scheme 2),[12, 20] PSBT and PSDTBT possess more blue-shifted absorption spectra and larger bandgaps due to the declining electron-donating strength of the donor unit by replacing the N-atom in the carbazole core with S-atom in the dibenzothiophene core.

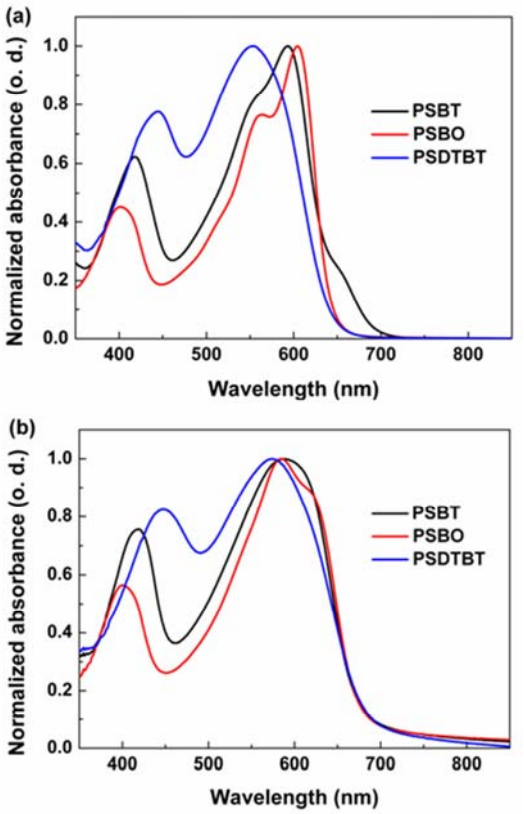

Fig. 2 Normalized UV-vis absorption spectra of the copolymers in chlorobenzene solution (a) and as pristine films (b).

Electrochemical properties

Cyclic voltammetry (CV) was employed to probe the electrochemical behaviors of these copolymers in thin film. CV measurements were conducted in a solution of 0.1 M tetrabutylammonium hexafluorophosphate (Bu_4NPF_6) in

Cite this: DOI: 10.1039/c0xx00000x

www.rsc.org/xxxxxx

ARTICLE TYPE

Table 1 Summary of molecular weights and optical and electrochemical properties of the copolymers

Polymers	M_n (kDa)[a]	PDI[a]	λ_{max} (nm) solution	λ_{max} (nm) film	E_g^{opt} (eV)[b]	T_d (°C)	HOMO (eV)[c]	LUMO (eV)[d]	μ_{hole} [cm^2 V^{-1} s^{-1}][e]
PSBT	7.6	1.3	418, 593	418, 588	1.81	315	-5.40	-3.59	$(1.8 \pm 0.1) \times 10^{-4}$
PSBO	7.7	1.8	402, 604	400, 585	1.82	309	-5.48	-3.66	$(4.6 \pm 0.2) \times 10^{-5}$
PSDTBT	5.3	1.7	445, 553	446, 574	1.82	320	-5.38	-3.56	$(1.3 \pm 0.1) \times 10^{-4}$

[a] The number-average molecular weight and polydispersity index measured by GPC. [b] The optical bandgap estimated from the onset of the film absorption spectrum. [c] Determined by onset oxidation potential of the CV curve from thin film. [d] $E_{LUMO} = E_{HOMO} + E_g^{opt}$. [e] Determined by the OFET method, the average mobilities are obtained from 5 devices.

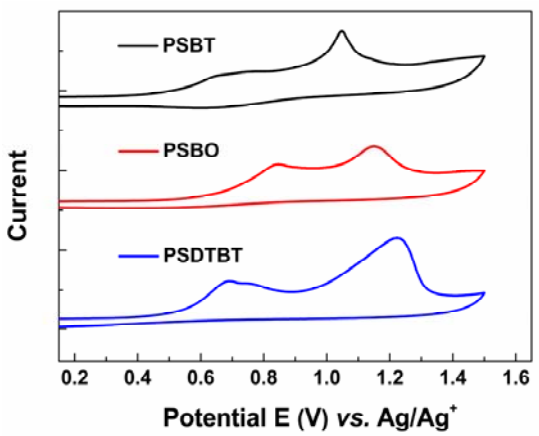

Fig. 3 Cyclic voltammograms of the polymer thin films on Pt electrode, performed in 0.1 M Bu_4NPF_6 acetonitrile solution at 100 mV s^{-1}.

acetonitrile at a scan rate of 100 mV/s, using a Pt disk coated with the polymer film, Pt wire, and Ag/Ag^+ (0.01 M $AgNO_3$ in anhydrous acetonitrile) as the working electrode, counter electrode, and reference electrode, respectively. The polymers were deposited onto the working electrode from a 3 mg/mL chloroform solution and dried under ambience prior to the measurements. Onset oxidation potentials of these three polymers deduced from the CV curves were found to be 0.54, 0.62 and 0.52 V for PSBT, PSBO and PSDTBT, respectively (Fig. 3). The onset oxidation potential ($E_{1/2}$ ox) of ferrocene was -0.06 V *versus* Ag/Ag^+ electrode under the same conditions. With an assumption that the redox potential of Fe/Fe^+ has an absolute energy level of -4.80 eV relative to vaccum,[23] the HOMO energy levels for PSBT, PSBO and PSDTBT were calculated to be -5.40, -5.48 and -5.38 eV, respectively (Table 1). These HOMO energy levels are within an ideal range to ensure good air-stability and are deeper-lying than those of their carbazole-cored analogues (Scheme 2).[12, 20] Therefore, larger attainable V_{oc}s in the final devices are expected because the V_{oc} of a PSC is proportional to the energy offset between the HOMO level of the donor material and the LUMO level of the acceptor material.[24] Compared to PSBT, the HOMO level of PSBO is lowered by 0.08 eV that benefits from the replacement of the BT unit by a stronger electron-withdrawing BO unit in the D-A copolymer. The LUMO energy levels were estimated by extracting the optical bandgaps from the corresponding HOMO levels, i.e. -3.59 eV for PSBT, -3.66 eV for PSBO and -3.56 eV for PSDTBT. These LUMO energy levels are sufficiently higher (> 0.3 eV) than the LUMO level of [6,6]-phenyl-C_{71}-butyric acid methyl ester ($PC_{71}BM$, *ca.* -4.30 eV) to overcome the exciton binding energy and thus guarantee an efficient exciton splitting and charge transfer.[2c]

Charge transport properties

Organic field-effect transistors (OFETs) were fabricated with the top-contact and bottom-gate geometry. A heavily *n*-doped Si wafer with a surface layer of 300 nm SiO_2 was employed as the substrate, which was treated by a drop of octadecyltrichlorosilane (OTS) in a vacuum oven at 130 °C for 22 h to form a self-assembled monolayer. Semiconductor polymers were spin-coated from their *o*-DCB/CB (v/v, 1/3) solutions at 800 rpm for 60 s onto the dielectric surface, and top-contact source/drain Au electrodes of about 50 nm thickness were deposited through a shadow mask under a vacuum of ~ 1×10^{-4} Pa. The channel width (W) and length (L) were 6.0 mm and 300 μm, respectively. Transistor behavior was observed when applying a negative gate voltages (V_{GS}), indicating that the polymer semiconductors had *p*-channel characteristics. The mobilities were calculated by plotting $I_{DS}^{1/2}$ with respect to V_{GS} (Fig. S1, ESI†) according to an equation in the saturation regime from the gate sweep:

$$I_{DS} = \mu C_i (W/2L) (V_{GS} - V_{TH})^2$$

where I_{DS} is the drain current, μ is the carrier mobility, C_i is the gate dielectric capacitance per unit area (SiO_2, 300 nm, C_i = 11 nF/cm^2), W and L are the semiconductor channel width and length, respectively, and V_{GS} and V_{TH} are gate voltage and threshold voltage, respectively.

Hole mobilities of pristine PSBT, PSBO and PSDTBT films deduced from the saturation regime were determined to be $(1.8 \pm 0.1) \times 10^{-4}$, $(4.6 \pm 0.2) \times 10^{-5}$ and $(1.3 \pm 0.1) \times 10^{-4}$ cm^2 V^{-1} s^{-1}, respectively. Although possessing a slightly lower molecular weight, a comparable value to PSBT has been observed for PSDTBT due to the insertion of two additional thiophene rings in the backbone units. However, the replacement of BT with BO

leads to a decrease in the carrier mobility (PSBT *vs*. PSBO).

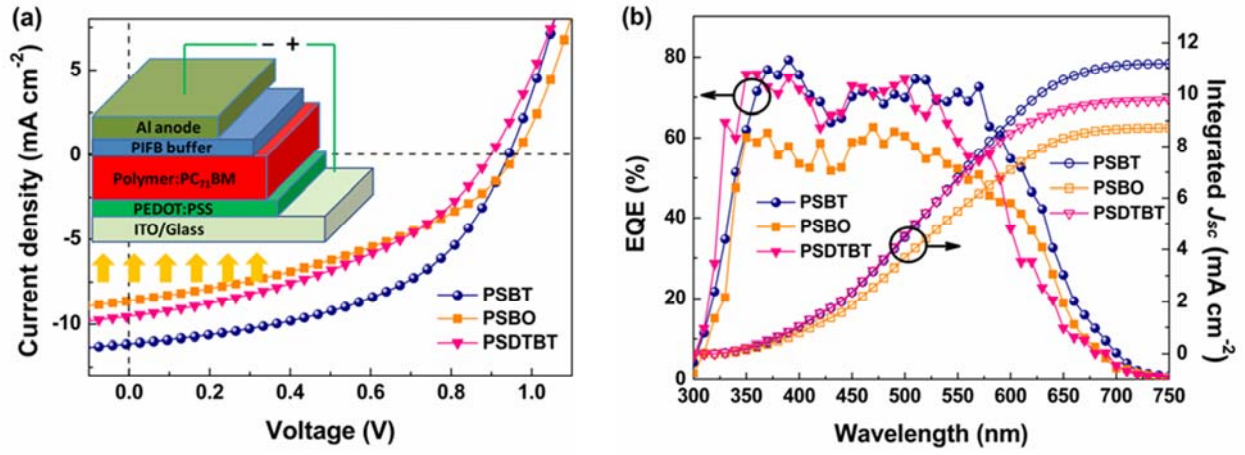

Fig. 4 (a) Current density-voltage (*J*-*V*) curves of the optimized PSCs based on polymer:$PC_{71}BM$ (1:3 in wt%) under the AM 1.5G (100 mW/cm^2) illumination. (b) EQE spectra (solid lines) and their integrated photocurrents (hollow lines) of the corresponding devices.

Table 2 Photovoltaic results of the BHJ PSCs based on the three copolymers

Polymers	D/A [a]	V_{oc} [V]	J_{sc} [mA cm^{-2}]	FF [%]	PCE_{max} (PCE_{ave})[c] [%]
PSBT	1:2.5[b]	0.96	9.66	47.7	4.41 (4.21 ± 0.10)
	1:3[b]	0.94	11.11	49.6	5.18 (5.12 ± 0.05)
	1:3.5[b]	0.95	9.14	50.9	4.41 (4.34 ± 0.05)
PSBO	1:3[b]	0.96	8.60	40.1	3.29 (3.22 ± 0.04)
PSDTBT	1:3[b]	0.90	9.50	41.3	3.52 (3.47 ± 0.04)

[a] Blend ratio of polymer:$PC_{71}BM$. [b] A mixed solvent of *o*-DCB:CB (1:3, v/v) is used. [c] The average PCEs with standard deviations are given in parentheses which are obtained from 8 devices.

Photovoltaic performance

Photovoltaic properties of the copolymers were investigated in conventional single-junction PSCs with the configuration of ITO/PEDOT:PSS/polymer:$PC_{71}BM$/PIFB/Al. The polyelectrolyte of poly[6,6,12,12-tetra(2-ethylhexyl)-6,12-dihydroindeno[1,2-b]fluorene-2,8-diyl-*alt*-2,5-bis(3-(dimethylamino)propoxy) benzene-1,4-diyl] (PIFB) is applied as a cathode buffer layer to improve the contact behavior between the active layer and the metal cathode[17b]. All active layers were spin-coated from a mixed solvent of *o*-dichlorobenzene:chlorobenzene (*o*-DCB:CB=1:3, v/v) without any additives. The current density-voltage (*J*-*V*) curves of the optimized PSCs measured under the AM 1.5G 100 mW cm^{-2} illumination are plotted in Fig. 4a, and the corresponding device parameters are summarized in Table 2. The optimized weight ratio of the polymer to $PC_{71}BM$ is 1:3 (Table 2). Through a systematic optimization, PSCs based on PSBT:$PC_{71}BM$ exhibit the best performance with a high V_{oc} of 0.94 V, a short-circuit current density (J_{sc}) of 11.11 mA cm^{-2}, a fill factor (FF) of 49.6%, and a respectable PCE of 5.18%. In comparison with its carbazole-based analogue of PCDCTBT (Scheme 2, PCE = 3.7%, V_{oc} = 0.80 V),[20] PSBT not only exhibits a superior PCE, but also a significantly enlarged V_{oc}. In contrast to polymer PSBT-H which has the same backbone skeleton of PSBT (PCE_{max} = 0.76% and V_{oc} = 0.64 V),[14] the results achieved herein have been considerably improved. The great V_{oc} difference between PSBT and its previous analogue (PSBT-H, Scheme 1) may be related with the more bulky side chains in addition to the cathode discrepancy.[25] In other words, it is found that the bulkiness of side chains can exert a significant influence on HOMO energy levels through the effect on molecular conformation/molecular interactions, i.e., more twisted polymer backbones have been shown to achieve lower-lying HOMO levels and therefore a high V_{oc} in devices.[25] In this work, PSBT and PSBT-H have the same backbone, but the steric hindrance for PSBT, imposed by the bulkier aryl side chains on the donor unit and additional aliphatic chains on the acceptor unit, would be greater than PSBT-H. Thus, the sterically induced twisting of the polymer backbone disrupts the π–conjugation between the donor and the acceptor moieties. Consequently, the delocalization of electrons from the donor unit to the acceptor unit become less favourable which leads to a lower HOMO level and a high V_{oc}.[26] The increased J_{sc} for the PSBT-based device can be attributed to its higher OFET mobility by an order of magnitude compared to the previous analogous polymer (1.8×10^{-4} *versus* 1.25×10^{-5} cm^2 V^{-1} s^{-1}).[14]

Cite this: DOI: 10.1039/c0xx00000x

www.rsc.org/xxxxxx

ARTICLE TYPE

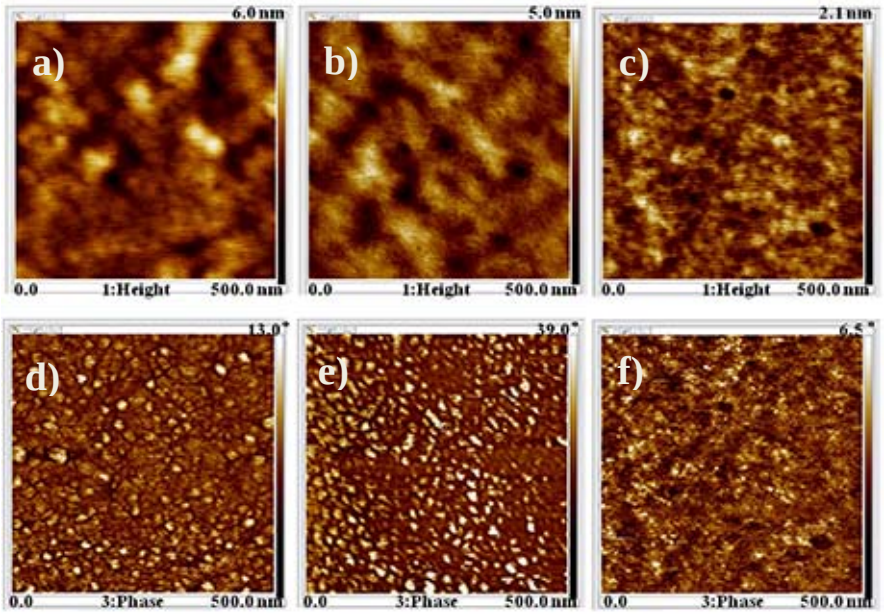

Fig. 5 Tapping-mode AFM topography (top) and phase (bottom) images of the blend thin films based on: a,d) PSBT:$PC_{71}BM$ (1:3, w/w%), b,e) PSBO:$PC_{71}BM$ (1:3, w/w%); c,f) PSDTBT:$PC_{71}BM$ (1:3, w/w%). The scan size is 0.5 μm × 0.5μm.

The hole mobility of a polymer is affected by its molecular weight and intermolecular interactions. Comparable molecular weights were determined for PSBT and PSBO. However, in terms of molecular structure, it is not unusual to observe that BT-containing polymers exhibit a higher hole mobility and larger J_{sc} values in comparison with BO-containing polymers.[8b] Moreover, the bulkier alkoxy side chains on the BO unit guarantee good solubility of PSBO, but they do not facilitate a good π-stacking. Therefore, the inferior values of hole mobility and J_{sc} are found for PSBO in relative to PSBT. As for PSBT and PSDTBT, a relatively higher molecular weight of PSBT (i.e., long polymer chains) is favorable for defect-free films, improved molecular π-π stacking, and inter-chain overlap between the polymers, all of which contributes to the higher hole mobility and larger J_{sc} values.[27] And it was found that this influence is especially notable for low molecular weight polymers (M_n < 10 kDa).[28] On the other hand, from the viewpoint of molecular structures of PSBT and PSDTBT, there should be a tradeoff between the effects of molecular backbone and side chains. The two additional thiophene units flanking on the BT in PSDTBT backbone help to relieve the steric hindrance between the neighboring six-membered aryl rings. Thus a more planar conjugated backbone would facilitate the chain-chain interactions among polymers. However, the additional thiophene rings usually decrease the solubility of the resulting polymers. In this regard, the longer and bulkier side chains of decyloxy on the BT unit can ensure the solution processability of the polymer, but their greater bulkiness would meanwhile cause unfavorable steric hindrance to keep the polymer chains from a close π-π stacking. Therefore, the superior hole mobility, J_{sc} and overall PCE of PSBT can be attributed to a good balance between the shorter alkyl side chains on its BT unit (favorable for intermolecular interactions, hole mobility, and J_{sc}) and the absence of two additional flanking thiophenes (unfavorable for intermolecular interactions, hole mobility, and J_{sc}, but favorable for V_{oc}).[26a, 29] These results highlight that the molecular backbone and side chains both exert significant effects on the properties of the polymer as well as the subsequent PSCs, and a subtle balance between solution processability and intermolecular interactions has to be established to obtain efficient PSCs.[29a] Briefly, it is general that shorter and less bulkier side chains facilitate molecular π-π stacking (ordering) and help to high performance PSCs when the solubility of the polymer and its miscibility with $PC_{71}BM$ are guaranteed.[30] Under the same device fabrication conditions, PSCs based on PSBO exhibit an optimal PCE of 3.29%, with V_{oc} = 0.96 V, J_{sc} = 8.60 mA cm^{-2} and FF = 40.1%. While PSCs based on PSDTBT exhibit a PCE of 3.52%, with V_{oc} = 0.90 V, J_{sc} = 9.50 mA cm^{-2} and FF = 41.3%. The V_{oc} values for devices based on these three polymers pose a declining order: PSBO > PSBT > PSDTBT, which is in agreement with their HOMO energy levels. On the other hand, the largest J_{sc} observed for PSBT and the smallest J_{sc} for PSBO are in accordance with their OFET mobilities.

To get more insights into the variations in hole mobility and J_{sc}, tapping-mode atomic force microscopy (AFM) was employed to probe the surface morphology of the blend films processed under the optimal PSC fabrication conditions. As shown in Fig. 5d, a well-developed interpenetrating network with finely diffused domains with sizes of 10-20 nm is observed for the PSBT-based

blend film, which enables a large interfacial area between the polymer donors and fullerene acceptors for efficient exciton dissociation, while providing a continuous percolating path for charge transport to the corresponding electrodes. So it is in accordance with the higher J_{sc} value of PSBT-based devices. While the phase separation and the domain size of PSDTBT-derived film are relatively not favorable for a high J_{sc} value of the corresponding device (Fig. 5f). For the film based on PSBO, large and irregular domains beyond an appropriate size are found (Fig. 5e), both of which are not beneficial for efficient exciton dissociation and charge transport. As for the comparison among the height topography images (Fig. 5a-c), a relatively rougher surface with a root mean square (RMS) roughness of 0.49 nm was found for PSBT-based film (Fig. 5a), as compared to those of 0.34 nm for PSBO (Fig. 5b) and 0.12 nm for PSDTBT (Fig. 5c). The introduction of two additional thiophenes in PSDTBT decreases the sterical hindrance between the donor and the acceptor units, which leads to a smoother surface for the PSDTBT-based film in comparison with the PSBT-based film.

To verify the reliability of the photovoltaic results, external quantum efficiencies (EQEs) of devices based on these three polymers were measured and the EQE spectra are shown in Fig. 4b. The EQE values of PSBT-based device are higher than those of PSDTBT-based device between 500 and 700 nm. PSBO-based device exhibits the lowest EQEs across the range from 300 to 600 nm. The EQE profiles agree well with the measured J_{sc} results, and errors between the J_{sc} values (calculated by integrating the EQE curves with the AM 1.5G spectrum) and those obtained from the *J-V* measurements are all within 3% (Fig. 4b).

Conclusions

We have provided an effective synthetic route to a dibenzothiophene-based ladder-type heptacyclic unit (SDCT), wherein it utilizes aryl ketones as the precursors of ester groups. A series of D-A copolymers incorporating SDCT as the donor unit and BT/BO derivatives as the acceptor units have been synthesized, characterized and applied for PSCs. Finally, a champion device based on PSBT exhibited a respectable PCE of 5.18% and a high V_{oc} of 0.94 V, all of which surpass the values from its carbazole-based analogue (PCE = 3.7%, V_{oc} = 0.80 V). Moreover, in comparison with the PCE of 0.76% and V_{oc} of 0.64 V for the polymer with the same backbone skeleton of PSBT, the photovoltaic performance achieved herein has been considerably improved. These results demonstrate that SDCT is a promising building block to construct D-A polymers for PSCs. In view of that the molecular weight of polymers exerts a significant effect on the device performance, even better results may be expected if PSBT with a larger molecular weight was obtained. Further work is underway to explore novel catalysts and methods for polymerization.

Experimental

Materials

All commercially available chemicals and reagents were used as received unless otherwise specified. THF was distilled over sodium/benzophenone, and other dry solvents were dried over molecular sieves. DTBT-OC_{10}, BT-OC_6 and BO-OC_8 units were synthesized according to previously reported procedures.[21] $PC_{71}BM$ (99%) was purchased from American Dye Source Inc. The synthesis of PIFB has been described by us previously.[17b, 31]

Instruments and measurements

^1H NMR and ^{13}C NMR spectra were acquired from a Bruker AVANCE-400 spectrometer with tetramethylsilane (TMS) as the internal reference, and the peaks are given in ppm relative to TMS. Molecular weights of the polymers were measured using the GPC method with polystyrene standards. UV-vis absorption spectra were recorded on a Perkin-Elmer Lamada 35 UV-vis spectrophotometer. TGA measurement was performed on a Netzsch STA449C platform. AFM was conducted in tapping mode with a Bruker Nanoscale V station. X-ray diffraction patterns of thin films deposited on the PEDOT:PSS/glass substrate were obtained with a Bruker D8 thin film diffractometer.

PSC fabrication and characterization

Devices with the structure of ITO/PEDOT:PSS/polymer:$PC_{71}BM$ /PIFB/Al were fabricated as follows: Indium-tin oxide (ITO) coated glass substrates (15 Ω/sq) were ultrasonically cleaned with detergent, deionized water, acetone and isopropanol in sequence, and then dried overnight in an oven. The precleaned substrates were subjected to UV-O_3 treatment for 15 min prior to use. Poly(3,4-ethylenedioxythiophene):poly(styrenesulfonate) (PEDOT:PSS, Baytron PVPAI-4083) was spin-cast onto the precleaned ITO at 3500 rpm for 60 s and then baked at 140 ^oC for 15 min in air. In a nitrogen-filled glovebox, a solution containing a mixture of polymer/$PC_{71}BM$ at different weight ratios (18 mg/mL) in a mixed *o*-DCB:CB (1:3, v/v) solvent was stirred overnight at 50 ^oC and filtered through a 0.45 μm filter before being spin-cast onto the PEDOT:PSS layer at 800 rpm for 60 s. Subsequently, a conjugated polyelectrolyte PIFB was introduced as an interlayer. The PIFB layer was spin-coated at 1500 rpm for 30 s from a methanol solution (0.3 mg/mL, containing 30 eq. of acetic acid). Finally, a layer of aluminum cathode was thermally deposited through a shadow mask under a high vacuum about 1×10^{-4} Pa. Each sample consists of eight independent devices with a fixed active area of 6 mm^2. Device characterization was performed under AM 1.5 G irradiation (100 mW cm^{-2}) on an Oriel sol3A simulator (Newport) with a NREL-certified silicon reference cell. The current density–voltage curves were tested by a Keithley 2440 source measurement unit. EQE spectra were measured on a Newport EQE measuring system.

Synthesis of monomers and polymers

Compound 2. To a cold suspension (0 ^oC) of 3,7-dibromodibenzo[b,d]thiophene (6.50 g, 19.0 mmol) and $AlCl_3$ (15.21 g, 6.0 eq.) in dry CS_2 (150 mL) was solwly added acetyl chloride (8.95 g, 6.0 eq.) over 30 min under nitrogen atmosphere. Then the stirring mixture was warmed and kept at reflux for 20 h. Upon cooling to room temperature, the reaction was quenched by slowly pouring the mixture into some crashed ice. The inorganic precipitate was dissolved with 2 M HCl, and the aqueous phase was extracted with dichloromethane (3 × 50 mL). The combined organic fractions were washed with water, saturated aq. $NaHCO_3$ and brine, dried over anhydrous $MgSO_4$, and concentrated by rotary evaporation. The resulting solid was purified by silica gel chromatography using 10% ethyl acetate in petroleum ether as

the eluent to afford the title compound as a pale yellow solid (8.1 g, 82%). ^{1}H NMR (400 MHz, $CDCl_3$, δ/ppm): 8.24 (s, 2H), 8.10 (s, 2H), 2.75 (s, 6H). HRMS (EI): *m/z* calcd for $C_{16}H_{10}Br_2O_2S$ [M^+] 423.8768, found 423.8770. Anal. calcd for $C_{16}H_{10}Br_2O_2S$ (%): C, 45.10; H, 2.37; Found (%): C, 45.44; H, 2.60.

Compound 3. A dioxane (60 mL) suspension of compound **2** (2.47 g, 5.80 mmol) was cooled with ice water under dark. A sodium hypochlorite solution (150 mL, available chlorine 5%) was added in portions and the stirred suspension was maintained at room temperature for 24 h before it was adjusted acid (pH = 1~2) with 1 M HCl. Collection by filtration and subsequent washing with water afforded the title compound as a white solid (2.45 g, 98%). ^{1}H NMR (400 MHz, DMSO-d_6, δ/ppm): 13.56 (s, 2H), 8.90 (s, 2H), 8.60 (s, 2H). ^{13}C NMR (100 MHz, DMSO-d_6, δ/ppm): 167.75, 142.99, 133.61, 131.25, 128.39, 124.74, 119.00. HRMS (EI): *m/z* calcd for $C_{14}H_6Br_2O_4S$ [M^+] 427.8354, found 427.8357. Anal. calcd for $C_{14}H_6Br_2O_4S$ (%): C, 39.10; H, 1.41; Found (%): C, 39.25; H, 1.26.

A 250 mL round-bottom flask was charged with the diacid (2.36 g, 5.49 mmol) obtained above, dioxane (60 mL), dichloromethane (80 mL) and drops of DMF (*ca.* 0.3 mL) before it was bubbled with nitrogen for 10 min, and then oxalyl chloride (2.85 g, 22.45 mmol) was syringed dropwise. The mixture was stirred overnight at room temperature and the volatiles were removed in vacuo. The resulting residue was suspended in dry MeOH (120 mL) and the mixture was heated at reflux for 8 h. Evaporation of the solvents afforded compound **3** as a white solid (2.44 g, 97% for two steps). ^{1}H NMR (400 MHz, $CDCl_3$, δ/ppm): 8.62 (s, 2H), 8.15 (s, 2H), 4.02 (s, 6H). HRMS (EI): *m/z* calcd for $C_{16}H_{10}Br_2O_4S$ [M^+] 455.8667, found 455.8666. Anal. calcd for $C_{16}H_{10}Br_2O_4S$ (%): C, 41.95; H, 2.20; Found (%): C, 41.99; H, 2.30.

Compound 4. In a 125 mL three-neck round-bottom flask equipped with a stir bar, a condenser and an inlet adapter, a mixture of compound **3** (2.21 g, 4.82 mmol), 2-thiopheneboronic acid (1.85 g, 3.0 eq.), 2 M aq. K_2CO_3 (19.3 mL, 8 eq.) and THF (60 mL) was degassed with nitrogen for 30 min, and then $Pd(PPh_3)_4$ (0.11 g, 0.02 eq.) was added quickly. The reactants were maintained at reflux under nitrogen for 24 h. Upon cooling, the mixture was poured into water, and extracted with ethyl acetate (120 mL × 3). The combined portions were dried over $MgSO_4$, filtered and concentrated *via* a rotary evaporator. The resulting crude product was purified by column chromatography on silica gel, eluting with ethyl acetate/petroleum ether (1/15) to get the title compound as a pale yellow solid (1.9 g, 85%). ^{1}H NMR (400 MHz, $CDCl_3$, δ/ppm): 8.60 (s, 2H), 7.97 (s, 2H), 7.40 (m, 2H), 7.11 (m, 4H), 3.82 (s, 6H). HRMS (MALDI): *m/z* calcd for $C_{24}H_{16}O_4S_3$ [M^+] 464.0211, found 464.0199. Anal. calcd for $C_{24}H_{16}O_4S_3$ (%): C, 62.05; H, 3.47; Found (%): C, 62.26; H, 3.51.

Compound 5. *n*-BuLi (10 mL, 2.5 M in hexane) was added dropwise to a solution of 1-bromo-4-hexylbenzene (5.93 g, 24.6 mmol) in anhydrous THF (20 mL) at -78 ^{o}C and under inert atmosphere. The stirred mixture was slowly warmed to -20 ^{o}C and then cooled again to -78 ^{o}C, wherein a degassed solution of compound **4** (1.9 g, 4.10 mmol) in THF (40 mL) was syringed dropwise over 40 min. When the addition was completed and another 10 min continued, the resulting mixture was slowly warmed to room temperature and stirred overnight, followed by quenching with a saturated NH_4Cl solution (15 mL). The organic layer was separated, and the aqueous phase was extracted with ethyl acetate for three times. The combined organic layer was washed with brine, dried over $MgSO_4$, filtered, and concentrated *via* a rotary evaporator to obtain a crude diol as a viscous oil, which could be directly used for the next step without further purification or purified by column chromatography on silica gel using 5% ethyl acetate in petroleum ether as the eluent to afford the title compound as a pale solid (3.01 g, 70%). ^{1}H NMR (400 MHz, $CDCl_3$, δ/ppm): 7.77 (s, 2H), 7.40 (s, 2H), 7.26 (m, 2H), 7.11 (m, 8H), 7.04 (m, 8H), 6.81 (m, 2H), 6.31 (d, J = 3.2 Hz, 2H), 3.40 (s, 2H), 2.65 (t, J = 7.6 Hz, 8H), 1.63 (m, 8H), 1.33 (br, 24H), 0.91 (m, 12H).

SDCT. The crude diol (3.01 g, 2.87 mmol) obtained above was dissolved in degassed dichloromethane (80 mL) and then a BF_3/Et_2O solution (4 mL) was syringed dropwise. After being stirred for 45 min, 50 mL of dry MeOH was added into the mixture to quench the reaction. The mixture was further stirred overnight, and then concentrated to give a viscous oil which was loaded onto a silica gel column and eluted with *n*-hexane to yield the title compound as a pale yellow solid (2.47 g, 85%). ^{1}H NMR (400 MHz, $CDCl_3$, δ/ppm): 7.89 (s, 2H), 7.84 (s, 2H), 7.31 (d, J = 4.8 Hz, 2H), 7.16 (d, J = 8.0 Hz, 8H), 7.03 (d, J = 8.4 Hz, 8H), 6.99 (d, J = 4.8 Hz, 2H), 2.53 (t, J = 7.6 Hz, 8H), 1.54 (m, 8H), 1.28 (m, 24H), 0.86 (t, J = 6.8 Hz, 12H). ^{13}C NMR (100 MHz, $CDCl_3$, δ/ppm): 157.19, 151.22, 142.17, 141.50, 140.51, 139.32, 136.37, 133.53, 128.61, 128.41, 127.95, 123.30, 119.21, 113.21, 62.72, 35.63, 31.79, 31.38, 29.25, 22.67, 14.16. HRMS (MALDI): *m/z* calcd for $C_{70}H_{76}S_3$ [M^+] 1012.5109, found 1012.5108. Anal. calcd for $C_{70}H_{76}S_3$ (%): C, 82.95; H, 7.56; Found (%): C, 82.64; H, 7.48.

Br-SDCT. NBS (0.81 g, 4.53 mmol) was added portion-wise to a solution of SDCT (2.0 g, 1.97 mmol) in $CHCl_3$ (60 mL). The stirring mixture was kept overnight under dark before removing the solvent *via* rotary evaporation. Chromatography purification of the resulting solid (SiO_2, hexane/ethyl acetate = 20/1) afforded the title compound as slight yellow powders (2.08 g, 90%). ^{1}H NMR (400 MHz, $CDCl_3$, δ/ppm): 7.89 (s, 2H), 7.80 (s, 2H), 7.15 (d, J = 8.4 Hz, 8H), 7.07 (d, J = 8.4 Hz, 8H), 7.03 (s, 2H), 2.57 (t, J = 7.6 Hz, 8H), 1.59 (m, 8H), 1.32 (m, 24H), 0.90 (t, J = 6.8 Hz, 12H). HRMS (MALDI): *m/z* calcd for $C_{70}H_{74}Br_2S_3$ [M^+] 1168.3319, found 1168.3314. Anal. calcd for $C_{70}H_{74}Br_2S_3$ (%): C, 71.78; H, 6.37; Found (%): C, 71.60; H, 6.42.

Sn-SDCT. To a stirred solution of Br-SDCT (1.0 g, 0.85 mmol) in anhydrous THF (35 mL) at -78 ^{o}C was added dropwise a 1.6 M solution of *t*-BuLi in hexane (2.1 mL). After being stirred at -78 ^{o}C for one additional hour, a THF (2 mL) solution of trimethyltin chloride (0.51 g, 2.55 mmol) was added dropwise. The resulting mixture was warmed up to room temperature and stirred overnight. After quenched with water, the organic phase was extracted with ethyl acetate for three times. The combined organic layer was dried over $MgSO_4$, filtered and concentrated *via* a rotary evaporator. Finally, recrystallization from ethanol afforded the distannyl monomer as a yellow solid (1.09 g, 96%).^{1}H NMR (400 MHz, $CDCl_3$, δ/ppm): 7.88 (s, 2H), 7.84 (s, 2H), 7.20 (d, J = 8.0 Hz, 8H), 7.07-7.02 (m, 10H), 2.56 (t, J = 7.6 Hz, 8H), 1.59 (m, 8H), 1.31 (m, 24H), 0.89 (t, J = 6.8 Hz, 12H), 0.39 (s, 18H). ^{13}C NMR (100 MHz, $CDCl_3$, δ/ppm): 158.78,

151.52, 146.43, 142.71, 142.45, 141.27, 139.17, 136.04, 133.35, 130.73, 128.29, 128.00, 119.29, 113.21, 62.16, 35.60, 31.75, 31.34, 29.23, 22.63, 14.12. -7.96. MS (MALDI): *m/z* calcd for $C_{76}H_{93}S_3Sn_2$ $[M+H]^+$ 1341.5, found 1341.4. Anal. calcd for $C_{76}H_{92}S_3Sn_2$ (%): C, 68.16; H, 6.92; Found (%): C, 68.31; H, 6.98.

PSBT. A 50 mL flame-dried round-bottom flask equipped with a stir bar, a condenser and an inlet adapter were charged with Sn-SDCT (0.43 g, 0.32 mmol), BT-OC_6 (0.16 g, 0.32 mmol) and dry toluene (10 mL). The solution was flushed with N_2 for 30 min, then $Pd_2(dba)_3$ (12 mg) and $P(o\text{-}tol)_3$ (16 mg) were added quickly. After bubbling the mixture with N_2 for another 30 min, it was heated to 100 °C for 2 days. Upon cooling to room temperature, the mixture was precipitated into methanol and filtered. The crude polymer was dissolved in chloroform, and filtered through a short silica gel column prior to being concentrated and precipitated into methanol again. The recovered polymer was purified by Soxhlet extraction sequentially with methanol, acetone, hexane and chloroform. The chloroform extracts were concentrated and precipitated into methanol. Collection by filtration and subsequent drying under vacuum yielded the polymer as a dark-purple solid (280 mg, 65%).^{1}H NMR (400 MHz, $CDCl_3$, δ/ppm): 8.58 (s, 2H), 7.98 (s, 4H), 7.30 (m, 8H), 7.12 (m, 8H), 4.15 (s, 4H), 2.59 (s, 8H), 1.96 (s, 4H), 1.61 (br, 12H), 1.35 (m, 32H), 0.93 (m, 18H). GPC (THF): M_n = 7.6 kDa, PDI = 1.3.

PSBO. Using a procedure similar to that described above for PSBT, Sn-SDCT (0.6 g, 0.45 mmol) and BO-OC_8 (0.24 g, 0.45 mmol) were copolymerized in dry toluene (15 mL) for 3 days to yield PSBO as purple black powders (300 mg, 48%). ^{1}H NMR (400 MHz, $CDCl_3$, δ/ppm): 8.48 (s, 2H), 7.98 (s, 4H), 7.28 (m, 8H), 7.10 (m, 8H), 4.22 (s, 4H), 2.58 (s, 8H), 2.07 (s, 4H), 1.60 (m, 12H), 1.34 (m, 36H), 0.93 (m, 18H). GPC (THF): M_n = 7.7 kDa, PDI = 1.8.

PSDTBT. Following the same procedure as that used for the synthesis of PSBT, PSDTBT was obtained as a purple black solid (253 mg, 52%) through the polymerization between Sn-SDCT (0.40 g, 0.30 mmol) and DTBT-OC_{10} (0.23 g, 0.30 mmol) in dry toluene (12 mL). ^{1}H NMR (400 MHz, $CDCl_3$, δ/ppm): 8.49 (br, 2H), 7.93 (br, 4H), 7.25 (br, 10H), 7.13 (br, 10H), 4.19 (s, 4H), 2.60 (s, 8H), 2.02 (s, 4H), 1.62 (br, 12H), 1.32 (br, 40H), 0.90 (br, 18H). GPC (THF): M_n = 5.3 kDa, PDI = 1.7.

Acknowledgments

This work was supported by National Science Foundation of China (Nos 51173186, 61325026), the National Basic Research 973 Program (No. 2011CB935904), and the CAS/SAFEA International Partnership Program for Creative Research Teams.

Notes and references

[a] *State Key Laboratory of Structural Chemistry, Fujian Institute of Research on the Structure of Matter, Chinese Academy of Sciences, 155 Yangqiao West Road, Fuzhou, Fujian 350002, P. R. China. Fax: +86-591-83721625; E-mail: qingdongzheng@fjirsm.ac.cn*

[b] *University of Chinese Academy of Sciences, Beijing 100049, P. R. China*

Electronic Supplementary Information (ESI) available: Transfer plots of the OFET devices based on PSBT, PSBO and PSDTBT. See DOI: 10.1039/b000000x/

1. (a) J. Chen and Y. Cao, *Acc. Chem. Res.*, 2009, **42**, 1709-1718; (b) P.-L. T. Boudreault, A. Najari and M. Leclerc, *Chem. Mater.*, 2010, **23**, 456-469; (c) Y. Li, *Acc. Chem. Res.*, 2012, **45**, 723-733; (d) X. Guo, A. Facchetti and T. J. Marks, *Chem. Rev.*, 2014, **114**, 8943-9021.
2. (a) C. W. Tang, *Appl. Phys. Lett.*, 1986, **48**, 183-185; (b) G. Yu, J. Gao, J. C. Hummelen, F. Wudl and A. J. Heeger, *Science*, 1995, **270**, 1789-1791; (c) J. Y. Kim, K. Lee, N. E. Coates, D. Moses, T.-Q. Nguyen, M. Dante and A. J. Heeger, *Science*, 2007, **317**, 222-225.
3. (a) Y. Sun, J. H. Seo, C. J. Takacs, J. Seifter and A. J. Heeger, *Adv. Mater.*, 2011, **23**, 1679-1683; (b) Z. Yin, Q. Zheng, S. Chen, D. Cai, L. Zhou, J. Zhang, *Adv. Energy Mater.*, 2014, **4**, 1301404; (c) F. Huang, H. Wu and Y. Cao, *Chem. Soc. Rev.*, 2010, **39**, 2500-2521; (d) Z. Yin, Q. D. Zheng, S-C. Chen, J. Li, D. Cai, Y. Ma, J. Wei, *Nano Research*, 2015, **8**, 456-468
4. (a) G. Li, V. Shrotriya, J. Huang, Y. Yao, T. Moriarty, K. Emery and Y. Yang, *Nat. Mater.*, 2005, **4**, 864-868; (b) L.-M. Chen, Z. Hong, G. Li and Y. Yang, *Adv. Mater.*, 2009, **21**, 1434-1449.
5. (a) Y.-J. Cheng, S.-H. Yang and C.-S. Hsu, *Chem. Rev.*, 2009, **109**, 5868-5923; (b) E. Wang, L. Hou, Z. Wang, S. Hellström, F. Zhang, O. Inganäs and M. R. Andersson, *Adv. Mater.*, 2010, **22**, 5240-5244; (c) X. Zhan and D. Zhu, *Polym. Chem.*, 2010, **1**, 409-419. (d) K. Li, Z. Li, K. Feng, X. Xu, L. Wang and Q. Peng, *J. Am. Chem. Soc.*, 2013, **135**, 13549-13557.
6. (a) J. D. Chen, C. Cui, Y. Q. Li, L. Zhou, Q. D. Ou, C. Li, Y. Li and J. X. Tang, *Adv. Mater.*, 2014, DOI: 10.1002/adma.201404535; (b) S.-H. Liao, H.-J. Jhuo, P.-N. Yeh, Y.-S. Cheng, Y.-L. Li, Y.-H. Lee, S. Sharma and S.-A. Chen, *Sci. Rep.*, 2014, **4**, 6813.
7. (a) W. Ma, C. Yang, X. Gong, K. Lee and A. J. Heeger, *Adv. Funct. Mater.*, 2005, **15**, 1617-1622; (b) G. Dennler, M. C. Scharber and C. J. Brabec, *Adv. Mater.*, 2009, **21**, 1323-1338.
8. (a) S. Beaupre and M. Leclerc, *J. Mater. Chem. A*, 2013, **1**, 11097-11105; (b) N. Blouin, A. Michaud, D. Gendron, S. Wakim, E. Blair, R. Neagu-Plesu, M. Belletête, G. Durocher, Y. Tao and M. Leclerc, *J. Am. Chem. Soc.*, 2008, **130**, 732-742.
9. (a) R. Qin, W. Li, C. Li, C. Du, C. Veit, H.-F. Schleiermacher, M. Andersson, Z. Bo, Z. Liu, O. Inganäs, U. Wuerfel and F. Zhang, *J. Am. Chem. Soc.*, 2009, **131**, 14612-14613; (b) Y. Deng, J. Liu, J. Wang, L. Liu, W. Li, H. Tian, X. Zhang, Z. Xie, Y. Geng and F. Wang, *Adv. Mater.*, 2014, **26**, 471-476.
10. (a) Y.-L. Chen, C.-Y. Chang, Y.-J. Cheng and C.-S. Hsu, *Chem. Mater.*, 2012, **24**, 3964-3971; (b) J.-S. Wu, S.-W. Cheng, Y.-J. Cheng and C.-S. Hsu, *Chem. Soc. Rev.*, 2015, **44**, 1113-1154.
11. Q. Zheng, S. Chen, B. Zhang, L. Wang, C. Tang and H. E. Katz, *Org. Lett.*, 2011, **13**, 324-327.
12. Y.-J. Cheng, J.-S. Wu, P.-I. Shih, C.-Y. Chang, P.-C. Jwo, W.-S. Kao and C.-S. Hsu, *Chem. Mater.*, 2011, **23**, 2361-2369.
13. J. Hou, H.-Y. Chen, S. Zhang, G. Li and Y. Yang, *J. Am. Chem. Soc.*, 2008, **130**, 16144-16145.
14. D. Cai, Q. Zheng, S.-C. Chen, Q. Zhang, C.-Z. Lu, Y. Sheng, D. Zhu, Z. Yin and C. Tang, *J. Mater. Chem.*, 2012, **22**, 16032-16040.
15. (a) S.-H. Chan, C.-P. Chen, T.-C. Chao, C. Ting, C.-S. Lin and B.-T. Ko, *Macromolecules*, 2008, **41**, 5519-5526; (b) Y. Zhang, J. Zou, H.-L. Yip, K.-S. Chen, J. A. Davies, Y. Sun and A. K. Y. Jen, *Macromolecules*, 2011, **44**, 4752-4758.
16. (a) B. Carsten, F. He, H. J. Son, T. Xu and L. Yu, *Chem. Rev.*, 2011, **111**, 1493-1528; (b) O. Inganäs, F. Zhang, K. Tvingstedt, L. M. Andersson, S. Hellström and M. R. Andersson, *Adv. Mater.*, 2010, **22**, E100-E116.
17. (a) Q. Zheng, S. K. Gupta, G. S. He, L.-S. Tan and P. N. Prasad, *Adv. Funct. Mater.*, 2008, **18**, 2770-2779; (b) Y. Ma, Q. Zheng, Z. Yin, D. Cai, S.-C. Chen and C. Tang, *Macromolecules*, 2013, **46**, 4813-4821.
18. Z. Fei, M. Shahid, N. Yaacobi-Gross, S. Rossbauer, H. Zhong, S. E. Watkins, T. D. Anthopoulos and M. Heeney, *Chem. Commun.*, 2012, **48**, 11130-11132.
19. X. Wang, P. Jiang, Y. Chen, H. Luo, Z. Zhang, H. Wang, X. Li, G. Yu and Y. Li, *Macromolecules*, 2013, **46**, 4805-4812.
20. J.-S. Wu, Y.-J. Cheng, M. Dubosc, C.-H. Hsieh, C.-Y. Chang and C.-S. Hsu, *Chem. Commun.*, 2010, **46**, 3259-3261.

21. (a) M. Helgesen, S. A. Gevorgyan, F. C. Krebs and R. A. J. Janssen, *Chem. Mater.*, 2009, **21**, 4669-4675; (b) J. Bouffard and T. M. Swager, *Macromolecules*, 2008, **41**, 5559-5562.
22. Y. Zhang, J. Zou, H.-L. Yip, K.-S. Chen, D. F. Zeigler, Y. Sun and A. K. Y. Jen, *Chem. Mater.*, 2011, **23**, 2289-2291.
23. J. Pommerehne, H. Vestweber, W. Guss, R. F. Mahrt, H. Bässler, M. Porsch and J. Daub, *Adv. Mater.*, 1995, **7**, 551-554.
24. M. C. Scharber, D. Mühlbacher, M. Koppe, P. Denk, C. Waldauf, A. J. Heeger and C. J. Brabec, *Adv. Mater.*, 2006, **18**, 789-794.
25. (a) X. Guo, N. Zhou, S. J. Lou, J. Smith, D. B. Tice, J. W. Hennek, R. P. Ortiz, J. T. L. Navarrete, S. Li, J. Strzalka, L. X. Chen, R. P. H. Chang, A. Facchetti and T. J. Marks, *Nat. Photonics*, 2013, **7**, 825-833; (b) S. Ko, E. T. Hoke, L. Pandey, S. Hong, R. Mondal, C. Risko, Y. Yi, R. Noriega, M. D. McGehee, J.-L. Brédas, A. Salleo and Z. Bao, *J. Am. Chem. Soc.*, 2012, **134**, 5222-5232.
26. (a) H. Zhou, L. Yang, S. Xiao, S. Liu and W. You, *Macromolecules*, 2009, **43**, 811-820; (b) I. McCulloch, M. Heeney, C. Bailey, K. Genevicius, I. MacDonald, M. Shkunov, D. Sparrowe, S. Tierney, R. Wagner, W. Zhang, M. L. Chabinyc, R. J. Kline, M. D. McGehee and M. F. Toney, *Nat. Mater.*, 2006, **5**, 328-333.
27. (a) J. J. Intemann, K. Yao, H.-L. Yip, Y.-X. Xu, Y.-X. Li, P.-W. Liang, F.-Z. Ding, X. Li and A. K. Y. Jen, *Chem. Mater.*, 2013, **25**, 3188-3195; (b) M. Tong, S. Cho, J. T. Rogers, K. Schmidt, B. B. Y. Hsu, D. Moses, R. C. Coffin, E. J. Kramer, G. C. Bazan and A. J. Heeger, *Adv. Funct. Mater.*, 2010, **20**, 3959-3965.
28. C. Müller, E. Wang, L. M. Andersson, K. Tvingstedt, Y. Zhou, M. R. Andersson and O. Inganäs, *Adv. Funct. Mater.*, 2010, **20**, 2124-2131.
29. (a) Z. Li, S.-W. Tsang, X. Du, L. Scoles, G. Robertson, Y. Zhang, F. Toll, Y. Tao, J. Lu and J. Ding, *Adv. Funct. Mater.*, 2011, **21**, 3331-3336; (b) L. Wang, D. Cai, Z. Yin, C. Tang, S.-C. Chen and Q. Zheng, *Polym. Chem.*, 2014, **5**, 6847-6856.
30. (a) J. Yuan, Z. Zhai, H. Dong, J. Li, Z. Jiang, Y. Li and W. Ma, *Adv. Funct. Mater.*, 2013, **23**, 885-892; (b) F. He, W. Wang, W. Chen, T. Xu, S. B. Darling, J. Strzalka, Y. Liu and L. Yu, *J. Am. Chem. Soc.*, 2011, **133**, 3284-3287; (c) H. Kim, B. H. Lee, K. C. Lee, G. Kim, J. Y. Yu, N. Kim, S. H. Lee and K. Lee, *Adv. Energy Mater.*, 2013, **3**, 1575-1580.
31. L. Wang, D. Cai, Q. Zheng, C. Tang, S.-C. Chen and Z. Yin, *ACS Macro Lett.*, 2013, **2**, 605-608.

Cite this: DOI: 10.1039/c0xx00000x

www.rsc.org/xxxxxx

ARTICLE TYPE

Graphical Abstract

Improved synthesis and photovoltaic performance of donor-acceptor copolymers based on dibenzothiophene-cored ladder-type heptacyclic units

Lixin Wang,[ab] Dongdong Cai,[a] Changquan Tang,[a] Meng Wang,[ab] Zhigang Yin[ab] and Qingdong Zheng*[a]

A ladder-type heptacyclic building block was synthesized with a high yield, and used for the construction of donor-acceptor copolymers with different π-spacers or different heteroatoms on the acceptor unit.